Journal of Solid State Chemistry **150,** 377–382 (2000)
doi:10.1006/jssc.1999.8610, available online at http://www.idealibrary.com on IDEAL®

Crystal Structures and Magnetic Properties of Rare-Earth Ultraphosphates, RP_5O_{14} (R = La, Nd, Sm, Eu, Gd)

J. M. Cole,*,[1] M. R. Lees,† J. A. K. Howard,‡ R. J. Newport,* G. A. Saunders,§ and E. Schönherr¶

*School of Physical Sciences, University of Kent at Canterbury, Canterbury, Kent, CT2 7NR, United Kingdom; †Department of Physics, University of Warwick, Coventry, CV4 7AL, United Kingdom; ‡Department of Chemistry, University of Durham, Durham, DH1 3LE, United Kingdom; §Department of Physics, University of Bath, Claverton Down, Bath, BA2 7AY, United Kingdom; ¶Max-Planck-Institut für Festkörperforschung, Heisenbergstrasse 1, 70569 Stuttgart, Germany

Received October 5, 1999; in revised form December 2, 1999; accepted December 13, 1999

The single-crystal X-ray structures of lanthanum, europium, and gadolinium ultraphosphate, RP_5O_{14} (R = rare-earth) are reported herein [monoclinic, $P2_1/c$, a = 8.8206(1), 8.7491(1), 8.7493(1) Å, b = 9.1196(2), 8.9327(1), 8.9189(1) Å, c = 13.1714(2), 12.9768(2), 12.9717(1) Å, β = 90.661(1), 90.534(1), 90.6682(3)°, respectively; Z = 4; $R1$ = 0.0250, 0.0346, 0.0270, respectively]. The structures are all type (I) compounds as classified by Bagieu-Beucher and Tranqui [*Bull. Soc. Fr. Miner. Cryst.* 93, 505 (1970)]. The minimum $R \ldots R$ separations are compared with all other structural reports of lanthanide ultraphosphates. Type (I) compounds have the lowest minimum $R \ldots R$ separation, which decreases with atomic number and appears not to perturb the optical properties of any rare-earth ultraphosphate. In each case, R is surrounded exclusively by eight oxygen atoms that form a distorted square antiprism. A P–O network holds together the three-dimensional structure. The magnetic susceptibilities of neodymium, samarium, and gadolinium ultraphosphate as a function of temperature are also reported along with corresponding magnetization measurements. All compounds exhibit a paramagnetic response, following Curie's law except in the regions where crystal field splittings are significant. © 2000 Academic Press

Key Words: **RP_5O_{14} structure; Paramagnetic; single-crystal X-ray diffraction.**

INTRODUCTION

Rare-earth ultraphosphates, RP_5O_{14}, have been the subject of considerable industrial interest on account of their high potential as lasing materials due to their desirable optical properties (1, 2). Such optical properties are strongly dependent upon the atomic structure of a material. In particular, the distance between rare-earth ions is important since there is a radial limit below which cross-relaxation of energy levels will occur, thereby causing depletion in efficiency of population inversion. Moreover, the extent of atomic/ionic shielding between rare-earth ions will further influence these effects and so precise knowledge of the spatial arrangement of these materials on an atomic level is crucial.

In view of this, the crystal structures of lanthanum, europium, and gadolinium ultraphosphate were determined. These structures are an addition to the partially established series of rare-earth ultraphosphate crystal structures that has been reported previously: CeP_5O_{14} (3), PrP_5O_{14} (4), NdP_5O_{14} (5), SmP_5O_{14} (6), TbP_5O_{14} (7), HoP_5O_{14} (8, 9), ErP_5O_{14} (10, 11), and YbP_5O_{14} (12). A structural determination of GdP_5O_{14} has also been reported (13), although the poor statistics obtained (e.g., $R = 0.103$) and the use of block refinement merited the full redetermination presented herein. Those structures are compared with the structures presented here. In particular, we were interested in ascertaining into which of the four structural types, as classified by Bagieu-Beucher and Tranqui (14) and Rzaigui and coworkers (3)[2] the subject compounds fall, given the prevalence of polymorphism in these systems (RP_5O_{14}, where R = Ce, Gd, Tb, Dy, Ho, Er (14)).

In a more general sense, ultraphosphates are one in the family of phosphates that comprise ortho-, pyro-, meta- and ultraphosphates given in order of decreasing rare-earth stochiometric content. In addition to similar optical effects, rare-earth metaphosphate compounds exhibit interesting magnetic properties (15) and therefore we were intrigued to discover the nature of the magnetic properties of the ultraphosphates. The magnetic susceptibilities as a function of temperature and field strength for NdP_5O_{14}, SmP_5O_{14}, and GdP_5O_{14} are therefore reported herein.

[1] To whom correspondence should be addressed. E-mail: jmc61@cam.ac.uk. Present address: Department of Chemistry, University of Cambridge, Lensfield Road, Cambridge, CB2 1EW, UK.

[2] Rzaigui and co-workers (3) report a "new" type of rare-earth ultraphosphate. They do not label this structural type explicitly as type (IV). However, since Bagieu-Beucher and Tranqui (14) use the type (I)–(III) classification, we simply adopt this scheme and extend it here to accommodate the CeP_5O_{14} structure.

0022-4596/00 $35.00

EXPERIMENTAL

X-Ray Crystallography

Single crystals were grown according to the procedure described by Danielmeyer and co-workers (16). A summary of crystal, data collection, and refinement parameters is given in Table 1. All experiments were carried out using a Siemens SMART-CCD diffractometer, which employed graphite monochromated Mo$K\alpha$ radiation (0.71073 Å). Each data collection nominally covered over a hemisphere of reciprocal space by a combination of three sets of exposures; each set had a different ϕ angle for the crystal setting and each exposure covered 0.3° in ω. The crystal-to-detector distance was 4.51 cm. Coverage of the unique set is more than 97% complete to at least 25° in θ. Crystal decay was monitored by repeating the initial frames at the end of data collection and analyzing the duplicate reflections. Cell parameters were refined using 512 reflections from all regions of reciprocal space, and data were reduced using the SAINT (17) program. A semiempirical absorption correction (via φ-scans) was applied in each case. All structures were solved by Patterson methods using SHELXS-86 (18) and subsequent difference Fourier syntheses and then refined by full-matrix least-squares methods on F^2 using SHELXL-93 (19). Atomic scattering factors were taken from "International Tables for Crystallography, Volume C, Mathematical, Physical and Chemical Tables" (20). Isotropic extinction corrections were applied in each structural refinement and positional and anisotropic displacement parameters were refined for all atoms.

TABLE 1
A Summary of Crystal, Data Collection, and Refinement parameters for the X-Ray Structures of Lanthanum, Europium, and Gadolinium Ultraphosphate

Compound	LaP_5O_{14}	EuP_5O_{14}	GdP_5O_{14}
Formula weight	517.76	530.81	536.10
Crystal system	Monoclinic	Monoclinic	Monoclinic
Space group	$P2_1/c$	$P2_1/c$	$P2_1/c$
a/Å	8.8206(1)	8.7491(1)	8.7493(1)
b/Å	9.1196(2)	8.9327(1)	8.9189(1)
c/Å	13.1714(2)	12.9768(2)	12.9717(1)
β/°	90.661(1)	90.534(1)	90.6682(3)
Cell volume (Å^3)	1059.44(3)	1014.13(2)	1012.17(2)
Z	4	4	4
Temperature (K)	145(2)	145(2)	145(2)
Total number of reflections	11388	9107	7084
Unique reflections	2428	2329	2332
Observed reflections $[I > 2\sigma(I)]$	2295	2270	2315
R_{int}	0.0643	0.0459	0.0454
Data/parameters	2424/182	2322/182	2325/182
Extinction parameter	0.0058(3)	0.0024(3)	0.0103(5)
$R1$ $[I > 2\sigma(I)]$	0.0250	0.0346	0.0270
w$R2$ $[I > 2\sigma(I)]$	0.0581	0.0826	0.0650
Goodness-of-fit on F^2	1.207	1.254	1.285

Magnetic Measurements

Measurements of dc magnetic susceptibility were made in the 5–350 K temperature range at 1000 Oe using a Quantum Design MPMS5 SQUID magnetometer. Magnetization versus field experiments were performed in an Oxford Instruments VSM in applied magnetic fields of up to 60 kOe at a constant temperature ($T = 2$ K).

RESULTS AND DISCUSSION

Refined atomic fractional coordinates with their equivalent isotropic atomic displacement parameters and bond lengths are given for all structures in Tables 2 and 3, respectively.

The magnetic susceptibilities as a function of temperature for neodymium, samarium, and gadolinium ultraphosphate are given in Figs. 1a–c, while Figs. 2a–c show their magnetization as a function of magnetic field at $T = 2$ K.

All three structures are type (I) rare-earth ultraphosphates as classified by Bagieu-Beucher and Tranqui (14) since they belong to the space group $P2_1/c$ and are isomorphous with each other and with all previously reported type (I) rare-earth ultraphosphate structures (4–7, 13). Several crystals of different morphologies were tested in each case but no evidence of polymorphism was found.

R–R Distances

A summary of all shortest $R \ldots R$ distances in rare-earth ultraphosphate structures is given in Table 4. The shortest $R \ldots R$ distances in each of the subject compounds are similar to each other and to those of type (I) structures reported previously. In accordance with the lanthanide contraction, the shortest $R \ldots R$ distances in all type (I) structures decrease with increasing atomic number. The shortest $R \ldots R$ distance increases from structure types (I), (II), (III), to (IV), respectively. Given that NdP_5O_{14} is a type (I) structure and yet still possesses excellent optical properties, we propose that the rare-earth ions in all rare-earth ultraphosphates are sufficiently far apart to preclude any decrease in the efficiency of population inversion.

R Coordination

In each case, the rare-earth ion is surrounded by eight oxygen atoms that form a distorted square antiprism. There is no direct R–P bonding and each of the oxygen atoms in the RO_8 polyhedra are shared exclusively with PO_4 tetrahedra. Average mean plane deviations for each square

TABLE 2

Atomic Fractional Coordinates (Å×10^5) and Equivalent Isotropic Atomic Displacement Parameters (Å^2×10^4) for Lanthanum, Europium, and Gadolinium Ultraphosphate X-Ray Diffraction Derived Structures

	x	y	z	U_{eq}
La(1)	77697(2)	69030(2)	99852(1)	52(1)
P(1)	100965(9)	99290(10)	70770(6)	64(2)
P(2)	74624(9)	104856(10)	83606(6)	60(2)
P(3)	81164(10)	125206(10)	100034(6)	60(2)
P(4)	72357(9)	105249(10)	116222(6)	60(2)
P(5)	49246(9)	100245(10)	132262(6)	59(2)
O(1)	91680(3)	61900(3)	115360(2)	102(5)
O(11)	91380(3)	61320(3)	84540(2)	106(5)
O(12)	91080(3)	106780(3)	79560(2)	112(5)
O(14)	113200(3)	90130(3)	77550(2)	96(5)
O(2)	71720(3)	91140(3)	89110(2)	118(5)
O(23)	72290(3)	119200(3)	89970(2)	92(5)
O(25)	63780(3)	108010(3)	74410(2)	97(5)
O(3)	103570(3)	81560(3)	99290(2)	93(5)
O(34)	70250(3)	118380(3)	108650(2)	96(5)
O(4)	72870(3)	90710(3)	111590(2)	117(5)
O(45)	58630(3)	108270(3)	123360(2)	101(5)
O(5)	58310(3)	61440(3)	87130(2)	109(5)
O(6)	78910(3)	41270(3)	100160(2)	116(5)
O(7)	57640(3)	62080(3)	111750(2)	97(5)
Eu(1)	77757(3)	69081(3)	99888(2)	55(1)
P(1)	100870(2)	99460(2)	70315(12)	70(3)
P(2)	74580(2)	104730(2)	83468(12)	68(3)
P(3)	81430(2)	125480(2)	100003(12)	56(3)
P(4)	72620(2)	105130(2)	116381(12)	65(3)
P(5)	49310(2)	100250(2)	132751(12)	62(3)
O(1)	91490(5)	61940(5)	114840(3)	98(9)
O(11)	91180(5)	61640(5)	84990(3)	102(9)
O(12)	91120(6)	107120(6)	79230(4)	160(10)
O(14)	113040(6)	90090(5)	77210(4)	149(10)
O(2)	72100(5)	90620(5)	88970(4)	114(9)
O(23)	72150(5)	119220(5)	90040(4)	106(9)
O(25)	63690(6)	107940(5)	74110(4)	143(10)
O(3)	103230(5)	81440(5)	99460(3)	93(9)
O(34)	70490(5)	118630(5)	108850(4)	120(9)
O(4)	73090(6)	90410(5)	111590(4)	125(9)
O(45)	58770(6)	108330(5)	123650(4)	143(10)
O(5)	58320(5)	61590(5)	87840(4)	105(9)
O(6)	79050(5)	41940(5)	100080(4)	103(9)
O(7)	57800(5)	62380(5)	111320(3)	100(9)
Gd(1)	77764(2)	69093(2)	99849(1)	75(1)
P(1)	100993(12)	99336(12)	70268(8)	79(2)
P(2)	74731(12)	104661(12)	83456(8)	79(2)
P(3)	81462(12)	125541(12)	99995(8)	79(2)
P(4)	72468(12)	105169(12)	116401(8)	79(2)
P(5)	49202(12)	100335(12)	132804(8)	73(2)
O(1)	91510(3)	61930(4)	114790(2)	119(6)
O(11)	91180(4)	61740(4)	85030(2)	121(6)
O(12)	91240(3)	106920(4)	79350(2)	116(6)
O(14)	113200(3)	89930(3)	77050(2)	110(6)
O(2)	72010(4)	90620(4)	89060(2)	123(6)
O(23)	72320(4)	119320(3)	89910(2)	109(6)
O(25)	63890(3)	107950(3)	74050(2)	102(6)
O(3)	103160(4)	81420(3)	99320(2)	103(6)
O(34)	70430(4)	118620(4)	108740(2)	120(6)
O(4)	73240(4)	90350(4)	111610(2)	133(6)
O(45)	58600(3)	108300(4)	123600(2)	113(6)
O(5)	58390(3)	61550(4)	87750(2)	122(6)
O(6)	79100(4)	42010(4)	100100(2)	128(6)
O(7)	57820(3)	62520(4)	111150(2)	115(6)

[O(11*A*)–O(3)–O(1)–O(6) and O(2)–O(4)–O(7)–O(5)] of the prism are 0.0065, 0.0468 Å (La); 0.0049, 0.0394 Å (Eu); 0.0052, 0.0476 Å (Gd), respectively. The distortion exists in three forms: (i) a tendency toward a diamond-like geometry rather than a square; (ii) the rare-earth ion in the cage is off-center and (iii) there is a slight tilt of each square plane with respect to the other (5.2° (La); 4.4° (Eu); 4.3° (Gd)]. The level of distortion appears to decrease with increasing atomic number, presumably because the rare-earth ion becomes more accommodating as it decreases in size according to the lanthanide contraction.

The geometry of the oxygen cage around the rare-earth in these structures was compared with those reported previously. As expected, all type (I) structures adopt a square

TABLE 3

Bond Distances (Å) for Lanthanum, Europium, and Gadolinium Ultraphosphate X-Ray Diffraction Derived Structures

Bond	LaP_5O_{14}	EuP_5O_{14}	GdP_5O_{14}
R(1)–O(7)	2.460(2)	2.378(4)	2.365(3)
R(1)–O(1)	2.462(2)	2.361(4)	2.358(3)
R(1)–O(11)	2.465(2)	2.366(4)	2.357(3)
R(1)–O(5)	2.479(2)	2.395(4)	2.394(3)
R(1)–O(2)	2.515(3)	2.437(4)	2.425(3)
R(1)–O(6)	2.535(3)	2.427(4)	2.419(3)
R(1)–O(4)	2.548(3)	2.473(5)	2.468(3)
R(1)–O(3)	2.554(2)	2.488(4)	2.481(3)
R(1)–*X*(1*A*)[a]	1.389(2)	1.350(4)	1.348(3)
R(1)–*X*(1*B*)[a]	1.293(3)	1.262(3)	1.259(3)
P(1)–O(11)^{i}	1.469(3)	1.467(5)	1.475(3)
P(1)–O(1)^{ii}	1.485(3)	1.485(5)	1.479(3)
P(1)–O(12)	1.610(3)	1.597(5)	1.611(3)
P(1)–O(14)	1.624(3)	1.619(5)	1.611(3)
P(2)–O(2)	1.470(3)	1.466(5)	1.469(3)
P(2)–O(25)	1.562(2)	1.562(5)	1.565(3)
P(2)–O(12)	1.562(2)	1.568(5)	1.558(3)
P(2)–O(23)	1.569(3)	1.566(5)	1.568(3)
P(3)–O(6)^{iii}	1.478(3)	1.484(5)	1.483(4)
P(3)–O(3)^{iv}	1.483(3)	1.479(5)	1.483(3)
P(3)–O(34)	1.621(3)	1.621(5)	1.620(3)
P(3)–O(23)	1.626(3)	1.620(5)	1.623(3)
P(4)–O(4)	1.461(3)	1.454(5)	1.463(3)
P(4)–O(14)^{iv}	1.565(2)	1.558(5)	1.568(3)
P(4)–O(45)	1.566(3)	1.569(5)	1.565(3)
P(4)–O(34)	1.568(3)	1.563(5)	1.567(3)
P(5)–O(7)^{v}	1.472(3)	1.471(4)	1.478(3)
P(5)–O(5)^{vi}	1.475(3)	1.472(5)	1.473(3)
P(5)–O(45)	1.618(3)	1.618(5)	1.621(3)
P(5)–O(25)^{vii}	1.623(3)	1.614(5)	1.620(3)

Note. (i)–(vii) refers to the symmetry transformations used to generate the equivalent second atom given in the bond description, where (i) $-x+2, y+1/2, -z+3/2$; (ii) $x, -y+3/2, z-1/2$; (iii) $x, y+1, z$; (iv) $-x+2, -y+2, -z+2$; (v) $-x+1, y+1/2, -z+5/2$; (vi) $x, -y+3/2, z+1/2$; (vii) $-x+1, -y+2, -z+2$.

[a] $X(1A)$ and $X(1B)$ relate to the position at the center of the prism squares defined by O(11*A*)–*O*(3)–*O*(1)–*O*(6) and O(2)–O(4)–O(7)–O(5), respectively.

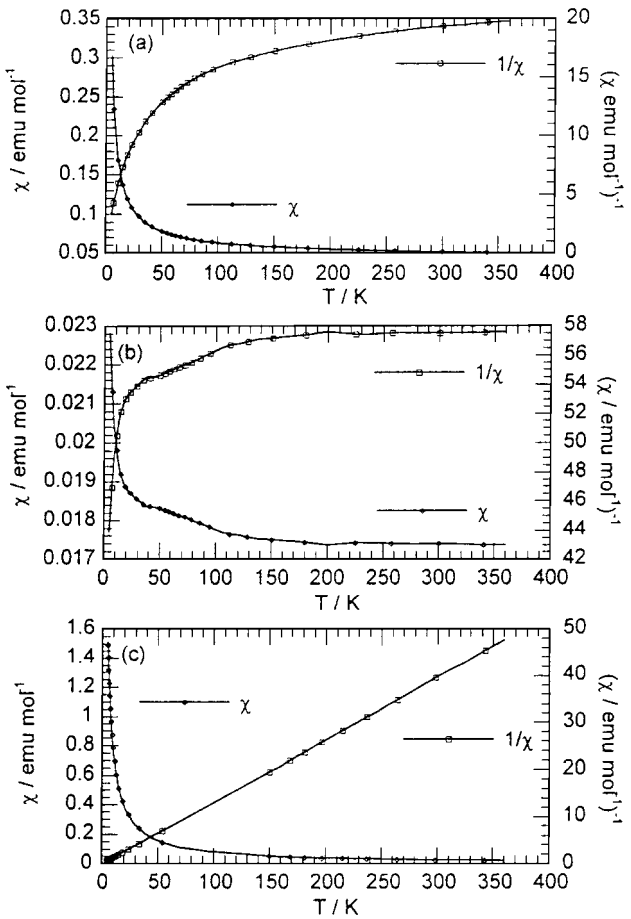

FIG. 1. The magnetic susceptibility and inverse magnetic susceptibility versus temperature for (a) NdP_5O_{14}, (b) SmP_5O_{14}, and (c) GdP_5O_{14}.

antiprism geometry[3] as does the other monoclinic [type (III)] rare-earth ultraphosphate form (average mean plane deviations of each prism square are 0.0045, 0.0415 Å (Nd); 0.0066, 0.0223 Å (Sm); 0.0453, 0.2250 Å (Er)). On the other hand, the orthorhombic type (II) structure is best described as a distorted bicapped trigonal prism while, in the triclinic type (IV) variety, oxygen atoms surround each rare-earth in a highly irregular manner.

P–O Network

All three structures possess five nonequivalent P positions and 14 nonequivalent O positions, thereby resulting in an O/P ratio of 14/5. This compares to values of 4 and 3 for analogous orthophosphate, RPO_4 and metaphosphate, $R(PO_3)_3$ compounds, respectively. Differences in the number of bridging oxygen atoms, Q^n, are responsible for these differences in O/P ratios. In the structures reported here, there exists a ratio of $3Q^2:2Q^3$ species as can be inferred from the bond geometry about each P atom, whereas the orthophosphate contains solely Q^4 species, i.e., isolated PO_4 tetrahedra, and in the metaphosphate, each PO_4 tetrahedron is a Q^2 species. The subject compounds therefore satisfy the definition of ultraphosphate species and are isotypic with those reported previously.

There is no direct P–P bonding in the network and so the packing arrangement of the structure is dictated by the geometry of the P–O bonding. An infinite chain of RP_4O_3 rings lie along both the crystallographic *a* and *b* axes. Each of these rings possess a pseudo-chair configuration as can be seen in Fig. 3. Two O–P–O branches emanate from either

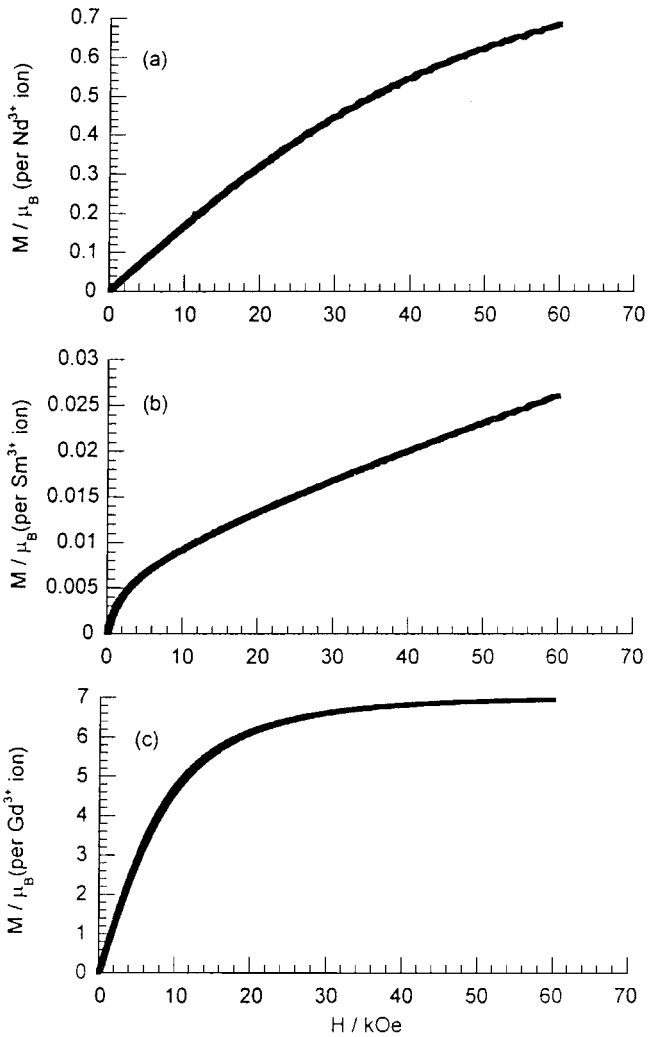

FIG. 2. The magnetization versus magnetic field (at $T = 2$ K) for (a) NdP_5O_{14}, (b) SmP_5O_{14}, and (c) GdP_5O_{14}.

[3] In the report concerning the structure of NdP_5O_{14} by Hong (5), the oxygen cage was described as a bicapped trigonal prism. However, we constructed a model according to the fractional coordinates reported and while one could approximate this shape around the rare-earth ion, it was clear from the geometry that a square antiprism described the cage better.

TABLE 4
A Summary of the Minimum *R* ... *R* Separation in All Reported Rare-Earth Ultraphosphate Structures

	Structure type	Shortest *R* ... *R* distance/Å	Data collection temperature	Space group	Reference
La	I	5.246(2)	145 K	$P2_1/c$	This work
Ce	IV	6.288	RT	$P1$	3
Pr	I	5.206	RT	$P2_1/c$	4
Nd	I	5.194	298 K	$P2_1/c$	5
Sm	I	5.175	RT	$P2_1/c$	6
Eu	I	5.174(4)	145 K	$P2_1/c$	This work
Gd	I	5.171(3)	145 K	$P2_1/c$	This work
Gd	I	5.153[a]	RT	$P2_1/c$	13
Tb	I	5.148[a]	RT	$P2_1/c$	7
Ho	II	5.574	RT	*Pnma*	8
Ho	III	5.714	RT	$C2/c$	9
Er	II	5.515	RT	*Pnma*	10
Er	III	5.70(1)	RT	$C2/c$	11
Yb	III	5.686	RT	$C2/c$	12

[a] In the original papers, the values of 5.902(1) Å (Gd) and 5.904 Å (Tb) were quoted. However, we have appraised the author's original data and their interpretation is in error since while these values exist they do not represent the *shortest* *R* ... *R* separations.

side of this ring and propagate along the crystallographic *c* axis joining to *R* and P groups from adjacent infinite chains, thereby resulting in a very rigid three-dimensional structure.

Magnetic Properties

The magnetic susceptibility as a function of temperature and of magnetic field was assessed for the compounds RP_5O_{14}, where R = Nd, Sm, and Gd. These materials were selected for testing since all three structures are type (I) rare-earth ultraphosphates and have been reported either previously (4–7, 13) or herein. The only other reported type (I) rare-earth ultraphosphate structures are those of LaP_5O_{14} and EuP_5O_{14} (this work) and these were not chosen because La^{3+} has no *f* electrons and so is diamagnetic while Eu^{3+} has an effective magnetic moment of zero due to the mutual cancellation of the spin and orbital angular momentum (assuming the $^7F_0$ ground state).

All three rare-earth ultraphosphate crystals tested gave a paramagnetic response. The response for GdP_5O_{14} obeys Curie's Law very well; this is consistent with the ($^8S_{7/2}$) ground state of Gd^{3+}, which has no orbital angular momentum and so is unaffected by crystal field effects. Fitting to $\chi = C/T + \chi_0$, where C is the Curie constant and χ_0 is a small temperature independent correction term to account for diamagnetism of the sample holder, gives a value of $g[j(j+1)]^{1/2}$ for Gd^{+3} of 7.97, which is in very good agreement with the predicted value of 7.94 (Ref. (21)).

Deviations from the characteristic $1/\chi$ versus T linear relationship were observed in the susceptibility data at $T < 150$ K in NdP_5O_{14} and throughout the temperature range in SmP_5O_{14}. Deviations from Curie's law are common in rare-earth salts due to the presence of crystal field effects. Such crystal field splittings are typically of the order of 10–100 cm^{-1} (21) and depend upon the local symmetry about the rare-earth ion (22): the lower the symmetry, the greater the crystal field splitting. These splitting energies correspond to a 14–144 K temperature range and so deviations from Curie's law can be expected below about 150 K. Indeed, the departure from Curie's law in NdP_5O_{14} begins at 150 K. The onset of such a deviation at this temperature reflects the distortion from the otherwise high symmetry of the square antiprism. In the case of NdP_5O_{14}, a satisfactory fit to the data was obtained by fitting it to an expression of the form $\chi = C/(T + \Delta) + \chi_0$, where the Δ term is introduced to allow for the effect of the splitting of the $2J + 1$ levels by the crystalline electric field (21). The fit yields $g[j(j+1)]^{1/2} = 3.34$ for Nd^{3+} and $\Delta \sim 30$ K. Both these values are consistent with expectations. In the case of SmP_5O_{14}, the crystal field effects are even more severe and affect the paramagnetic response across the whole temperature range measured (5–300 K). This is a consequence of the presence of the low-lying excited sates with higher values of J than the ground state, $^6H_{5/2}$, at room temperature. No

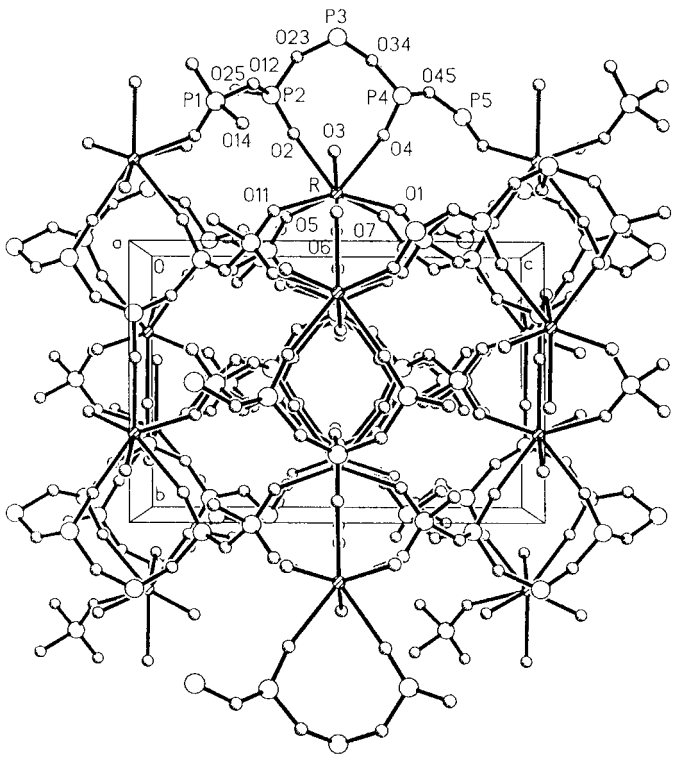

FIG. 3. The structural arrangement of NdP_5O_{14}, SmP_5O_{14}, and GdP_5O_{14}, viewed in the [100] plane.

fits to the data using a simple Curie expression are possible in this case.

The display of paramagnetism is a further indication to us that the rare-earth ions are sufficiently far apart from each other that no interaction between them is occurring. Furthermore, the fact that GdP_5O_{14} is paramagnetic suggests that all rare-earth ultraphosphates are paramagnetic since GdP_5O_{14} possesses the shortest minimum $R \ldots R$ separation (see Table 4) except for type (I) TbP_5O_{14}, (Tb being the smallest rare-earth ion permitted to exist as a type (I) ultraphosphate (14)) in which R–R is only marginally shorter than in the present case.

The measurements of magnetization (M) as a function of magnetic field (H) reveal that the magnetic response of all the compounds tested are reversible with no hysteresis. For GdP_5O_{14} the M versus H curve has a Brillouin form typical of a paramagnetic. There is a tendency toward saturation for H/T above 20 kOe/K and a value of 7 μ_B/Gd^{3+} ion (μ_B = Bohr magneton). These results agree well with previous measurements on paramagnetic Gd salts (21). For NdP_5O_{14} the crystal field effects reduce the moment on each Nd^{3+} ion to 0.7 μ_B at 60 kOe, although the M–H curve still has the conventional field dependence. For SmP_5O_{14} the curvature of the M versus H response decreases as the magnetic field is increased. The moment per Sm^{3+} ion is only 0.025 μ_B at 60 kOe. This underlines the strong effects of crystal fields in this material.

CONCLUSIONS

The X-ray diffraction derived structures reported herein are revealed as type (I) rare-earth ultraphosphates according to the classification by Bagieu-Beucher and Tranqui (14). The rare-earth ions lie in a cage of eight oxygen atoms that form a distorted square antiprism. This distortion appears to exacerbate the crystal field effects in the magnetic data. The square antiprism is the best described geometry about R^{3+} for all monoclinic (type (I) and type (III)) rare-earth ultraphosphates. The minimum separation observed between rare-earth ions is lowest for type (I) structures. This $R \ldots R$ distance is similar for all type (I) species although we do observe a slight decrease with increasing atomic number in accordance with the lanthanide contraction. Given that NdP_5O_{14} has a type (I) structure and possesses excellent optical properties, we propose that no rare-earth ultraphosphate compounds are affected significantly by this proximity of R^{3+} ions. Furthermore, the magnetic measurements on neodymium, samarium, and gadolinium ultraphosphates reported here display a paramagnetic response which indicates that there is no interaction between the rare-earth ions. The paramagnetic response obeys Curie's law except where crystal field splitting effects are significant. We postulate that all rare-earth ultraphosphate compounds are paramagnetic on the basis of our results. Each RO_8 polyhedron is linked to another via an infinite three-dimensional rigid P–O framework.

ACKNOWLEDGMENTS

The authors thank the EPSRC for financial support (J.M.C.) and Durham University for a Sir Derman Christopherson Foundation Fellowship (J.A.K.H.).

REFERENCES

1. H. G. Danielmayer and H. P. Weber, *J. Quant. Electron* **8,** 805 (1972).
2. Z. Mazurak, W. Ryba-Romanowski, and B. Jeżowska-Trzebiatowska, *J. Lumin.* **17,** 401 (1978).
3. M. Rzaigui, N. Kbir Ariguib, M. T. Averbuch-Pouchot, and A. Durif, *J. Solid State Chem.* **52,** 61 (1984).
4. S. Liu, G. Hong, and N. Hu, *Acta Phys. Sinica* **40,** 64 (1991).
5. (a) H. Y-P. Hong, *Acta Crystallogr. Sect. B* **30,** 468 (1974). (b) K.-R. Albrand, R. Attig, J. Fenner, J. P. Jeser, and D. Mootz, *Mater. Res. Bull.* **9,** 129 (1974).
6. D. Tranqui, M. Bagieu, and A. Durif, *Acta Crystallogr Sect. B* **30,** 1751 (1974).
7. Y. Lin, N. Hu, M. Wang, and E. Shi, *Acta Chimica Sinica* **40,** 211 (1982).
8. (a) A. Durif, *Bull Soc. Fr. Miner. Crist.* **94,** 314 (1971). (b) D. Tranqui, M. Bagieu-Beucher, and A. Durif, *Bull. Soc. Fr. Miner. Crist.* **95,** 437 (1972).
9. M. Bagieu, I. Tordjman, A. Durif, and G. Bassi, *Cryst. Struct. Comm.* **3,** 387 (1973).
10. A. Katrusiak and F. Kaczmarek, *Cryst. Res. Technol.* **30,** 501 (1995).
11. B. Jeżowska-Trzebiatowska and Z. Mazurak, *Acta Crystallogr Sect. B* **36,** 1639 (1980).
12. H. Y.-P. Hong and J. W. Pierce, *Mater. Res. Bull.* **9,** 179 (1974).
13. Y. Lin, N. Hu, Q. Zhou, and S. Wu, *Chinese J. Appl. Chem.* **1,** 33 (1983).
14. M. Bagieu-Beucher and D. Tranqui, *Bull. Soc. Fr. Miner. Cryst.* **93,** 505 (1970).
15. G. Carini, G. D'Angelo, G. Tripodo, A. Fontana, F. Rossi, and G. A. Saunders, *Europhys. Lett.* **40,** 435 (1997).
16. H. G. Danielmeyer, J. P. Jeser, E. Schönherr, and W. Stetter, *J. Crystal Growth* **22,** 298 (1974).
17. Siemens Analytical X-ray Instruments, "SAINT, Version 4.050." Siemens Analytical X-ray Instruments, Inc., Madison, WI, 1995.
18. G. M. Sheldrick, *Acta Crystallogr. Sect. A* **46,** 467 (1990).
19. G. M. Sheldrick, "SHELXL-93. Program for the Refinement of Crystal Structures Using Single Crystal Diffraction Data." University of Göttingen, Germany, 1993.
20. A. J. C. Wilson (Ed.), "International Tables for Crystallography, Volume C, Mathematical, Physical and Chemical Tables, Tables 4.2.6.8 and 6.1.1.4., pp. 219–222 and 500–503." Kluwer, Dordrecht, 1992.
21. B. I. Bleaney and B. Bleaney, "Electricity and Magnetism," Chap. 20. Oxford University Press, Oxford, 1957.
22. B. G. Wybourne, "Spectroscopic Properties of Rare Earths," Chap. 6. Interscience, New York, 1965.